Environmental Earth Sciences (2019) 78:19
https://doi.org/10.1007/s12665-018-8025-y

ORIGINAL ARTICLE

Downwind aeolian sediment accumulations associated with lake-level variations of the Qinghai Lake during the Holocene, Northeastern Qinghai–Tibetan Plateau

Xiang-Jun Liu[1,2] · Lu Cong[2,3] · Fuyuan An[1,2] · Xiaodong Miao[4] · Chongyi E[5]

Received: 28 February 2018 / Accepted: 19 December 2018 / Published online: 2 January 2019

Abstract

Many lakes in the Qinghai–Tibetan Plateau (QTP) have aeolian sands distributed in their downwind shores. However, it has been rarely systemically investigated on whether the downwind dune sand and lake evolved in association with each other or they evolved independently. Here we take the well known Qinghai Lake and its downwind sand area as a case study to investigate the issue of water–sand interaction. Grain size, magnetic susceptibility and geochemical data along with optically stimulated luminescence (OSL) ages suggest that the downwind eastern shore sandy lands co-varied with the lake level fluctuations (or lake extension changes) of the Qinghai Lake during the Holocene epoch. During the early Holocene lake lowstands (11–9 ka, ka is 1000 years), vast areas of exposed lacustrine sediments were eroded by prevailing westerly winds, therefore, causing sand to accumulate at the eastern shore bajada areas along the west piedmonts of the Riyue Mount, and to expand along the Daotang River valley. In contrast, during the mid to late Holocene lake highstands (7–1.2 ka), eastern shore dune sands were largely stabilized, and loess accumulated and even paleosol developed, leading to substantial shrinkage of the eastern shore sandy lands. In addition, using GIS tool, we reconstructed the spatial extensions of the lake during highstand (Mid-Holocene) and lowstand (Early Holocene), and eastern shore desert range of early Holocene. As a result, this study indicates a close connection between the lakes in QTP and the aeolian sands downwind.

Keywords Aeolian sediments · Lake level variations · Qinghai Lake · Qinghai–Tibetan Plateau · Holocene

Introduction

Dusts on the Qinghai–Tibetan Plateau (QTP) can be deflated into the atmosphere and transported to the low altitude areas downwind (Fang et al. 2004). Hence, sand dunes and Gobi-desert regions in QTP supply large amounts of potential silt-sized sediments for the downwind sedimentary regions, such as the Chinese Loess Plateau (CLP) (Fang et al. 2004; Kapp et al. 2011; Pullen et al. 2011; Liu et al. 2017). Therefore, understanding the aeolian system of the QTP not only has local significance for the paleoclimate reconstruction, but also is important for the large-scale, e.g., regional, correlation to the CLP.

Closed lakes are the sedimentary sinks for the inflow drainages in QTP, and many lakes in QTP have sand dunes distributed in their downwind shores. However, it is rarely investigated whether the downwind shore sands evolved in association with the lakes, or they are evolved independently. Here we use the Qinghai Lake and its downwind dune sand as a case study to investigate whether the lake

Electronic supplementary material The online version of this article (https://doi.org/10.1007/s12665-018-8025-y) contains supplementary material, which is available to authorized users.

✉ Xiang-Jun Liu
xjliu@isl.ac.cn; xiangjunliu@126.com

[1] Key Laboratory of Comprehensive and Highly Efficient Utilization of Salt Lake Resources, Qinghai Institute of Salt Lakes, Chinese Academy of Sciences, Xining 810008, China

[2] Qinghai Provincial Key Laboratory of Geology and Environment of Salt Lake, Qinghai Institute of Salt Lakes, Chinese Academy of Sciences, Xining 810008, China

[3] University of Chinese Academy of Sciences, Beijing 100049, China

[4] School of Resources and Environmental Sciences, Linyi University, Linyi 276000, China

[5] School of Geography, Qinghai Normal University, Xining 810008, China

and its downwind aeolian sands were linked or not during the Holocene epoch.

Aeolian sediments surrounding the Qinghai Lake are usually 1–3 m thick of loess mantle on the top of bedrocks, alluvium, river terraces or paleoshoreline gravels. They can be easily identified at both sides of the highways around the lake. Previous dating results suggest that loess surrounding the Qinghai Lake accumulated since the last deglaciation (Chen et al. 1990, 1991; Madsen et al. 2008; Liu et al. 2012; Lu et al. 2010, 2015; Yuan et al. 1990). On the other hand, researches on lake level variations reported that early Holocene lake level of the Qinghai Lake was quite low: lake water was less than 10 m deep (Kelts et al. 1989; Zhang et al. 1994; Yu and Kelts 2002a; Yu 2005; Liu et al. 2015; Wang et al. 2015), compared to modern average of ~22 m; the lake level rose substantially after ~8 ka, reached the Holocene highest stand at ~5 ka (about 9.1 m higher than modern level), and declined during the past 2 ka (Liu et al. 2015).

On the eastern margin of the Qinghai Lake, two patches of mobile dunes (Fig. 1b) spread from north of Gahai lagoon to south Haiyan Bay, and another small patch of active dunes distributed to the southeast of the lake, located at the source region of Daotang River. These three patches of active sand dunes were called eastern shore sandy lands, with a modern area of ~475 km^2 (Wang et al. 2017). Up to present, only a few preliminary studies on when and how the eastern shore sandy lands formed. Xu and Xu (1983) proposed that the formation of eastern shore sandy lands was associated with the recessions of Qinghai Lake during Holocene epoch. They thought the Holocene recession of the lake exposed lacustrine sediments which were eroded by prevailing westerly winds, making the medium to coarse sands accumulated downwind. Yao et al. (2015) regarded that modern mobile dunes at the eastern shore of Qinghai Lake were the results of mechanical disruptions of in situ ancient sands after the surface grass turfs were damaged. Wang et al. (2017) proposed that Qinghai Lake shrunk substantially during last glacial maximum (LGM) and early Holocene, thereby making large areas of lake floors exposed. The exposed lacustrine sediments were eroded by westerly winds, and sands accumulated at the west piedmonts of Riyue Mount, thereby making the eastern shore sands spread out (purple dashed line in Fig. 1b) from northeastern lake shore to the southeastern lake drainage where Daotang River originated. Up to date, it is still inconclusive on: (1) when and how the eastern shore sandy lands formed, (2) how big its spatial extent variations through time, and (3) the relationships between the Qinghai Lake and its downwind eastern shore sandy lands.

In this study, we combined the ages of aeolian deposit reported within eastern shore sandy lands, the reported Holocene lake level variation curves and reconstructed early and middle Holocene lake extensions, to explore the relationships between the Qinghai Lake and the downwind eastern shore sandy lands during the Holocene epoch. We also investigated two representative aeolian deposit sections within the eastern shore sandy lands.

Study area

Qinghai Lake, the largest inland closed lake in China, locates on the northeastern QTP at the elevation of ~3200 m above sea level (Fig. 1a). Its vast size and proximity to two major climate systems-Westerlies and Asian Summer Monsoon (ASM)-makes it sensitive to large-scale climate changes (Madsen et al. 2008; Liu et al.

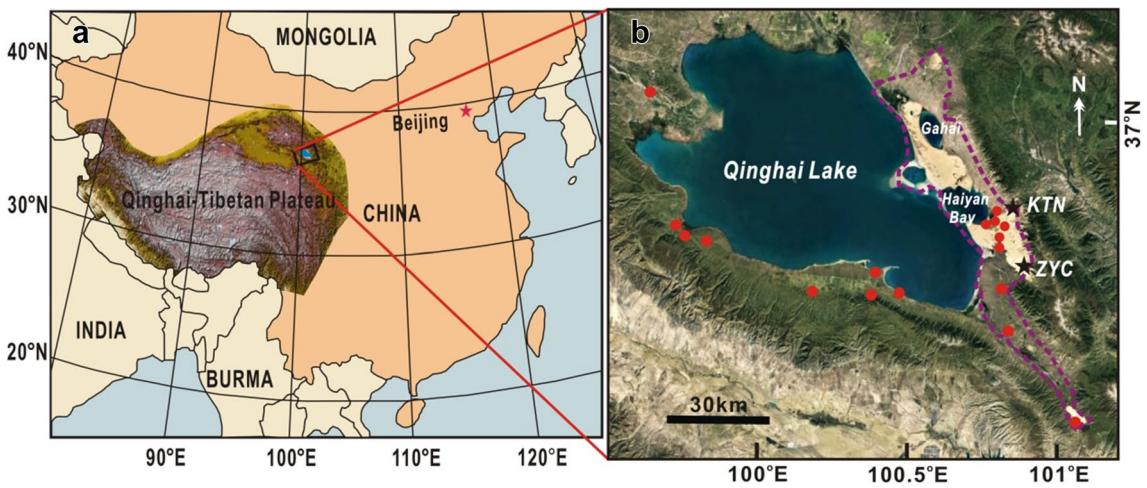

Fig. 1 **a** Map showing the location of Qinghai Lake, northeastern Qinghai–Tibetan Plateau; **b** satellite image of Qinghai Lake and surrounding areas. Red dots are aeolian profiles reported by previous studies; filled black five-point stars are KTN and ZYC sections in this study; purple dashed line represents aeolian sand areas in early Holocene lake lowstand between 11 and 9 ka

2015; Rhode et al. 2010). It was extensively investigated by scientists from China and abroad for the late Quaternary paleoenvironmental changes (Zhang et al. 1994; Yu and Kelts 2002a, b; Shen et al. 2005; Madsen et al. 2008; Liu et al. 2010; Rhode et al. 2010; An et al. 2012; Chen et al. 2016; Li and Liu 2014, 2017; Li et al. 2018). Recent research of lacustrine sediments reported that the climate of Qinghai Lake was dominantly controlled by westerlies during the last glaciation, and was predominantly influenced by the ASM during the Holocene (An et al. 2012). Aeolian sediments at the western and southern margins of the Qinghai Lake were thought to be deposited independent of the lacustrine sediments, and these aeolian sediments were also investigated for their deposition ages and preserved paleoenvironmental information (Chen et al. 1991; Lu et al. 2010, 2015; Liu et al. 2012; Zeng et al. 2017) (Fig. 1b). However, aeolian sediments at the eastern shore of the Qinghai Lake are thought to be coupled with the evolutions of Qinghai Lake because exposed lacustrine sediments may be the important source for downwind aeolian sands (Xu and Xu 1983; Wang et al. 2017).

Qinghai Lake is now a brackish lake with salinity of 14 g/L, and the lake area is ~4400 km^2. The average water depth is ~22 m, and the maximum depth is approximately 30 m. It is located at the junction of the ASM and the Westerlies, sensitive to these two atmospheric circulation changes, and is the ideal place to investigate past ASM–Westerlies interactions (An et al. 2012). Observational data from the Gangcha meteorological station on the north margin of the lake report that the annual mean temperature is − 0.3 °C, with the highest monthly mean temperature of 10.9 °C (July), and the lowest monthly mean temperature of − 13.5 °C (January) (Ma 1998). The annual mean precipitation is ~373 mm (An et al. 2012), and the annual mean evaporation in the Qinghai Lake is ~900 mm (Li et al. 2016). The main tributaries of Qinghai Lake are the Buha River, contributing about half of the annual water input to Qinghai Lake, the Shaliu River, the Haergai River, the Quanji River and the Heima River (Li et al. 2007).

Three patches of mobile sands, called eastern shore sandy lands, distributed along the eastern shore of Qinghai Lake. Two large patches of sand dunes distribute between Qinghai Lake and Riyue Mount, and another small patch of sand dunes locate at the source region of Daotang River (Fig. 1b). Sand dunes within the sandy lands are composed of transverse dunes and pyramid dunes. Transverse dunes mostly distribute near the lake, while pyramid dunes distribute near the mountain front. Sand islands and sand dams distribute along the eastern lake margin and spread westward into the lake, and aeolian sands also deposited underwater within the Haiyan Bay (Wang et al. 2017; Xu and Xu 1983).

Sampling section description and data measurements

The Zhongyangchang (ZYC) aeolian section was investigated and sampled for this study. The Ketu-North (KTN) aeolian section was investigated and reported by Lu et al. (2015), and we used their published data in this study. These two sections locate at the easternmost of the sand dunes, near the Riyue mount and at the distal side of pyramid dunes. The ZYC aeolian section (36°38′N, 100°52′E) lies to the southeast of Qinghai Lake (Fig. 1b). The exposed ZYC section is ~1.5 m thick, and can be divided stratigraphically into aeolian sand, loess, paleosol, and a modern soil from bottom to top (Fig. 2). The top ~0.3 m is loose modern soil, with sediments coarser than the underlying loess and paleosol. The paleosol and loess occur from a depth of 0.3 to

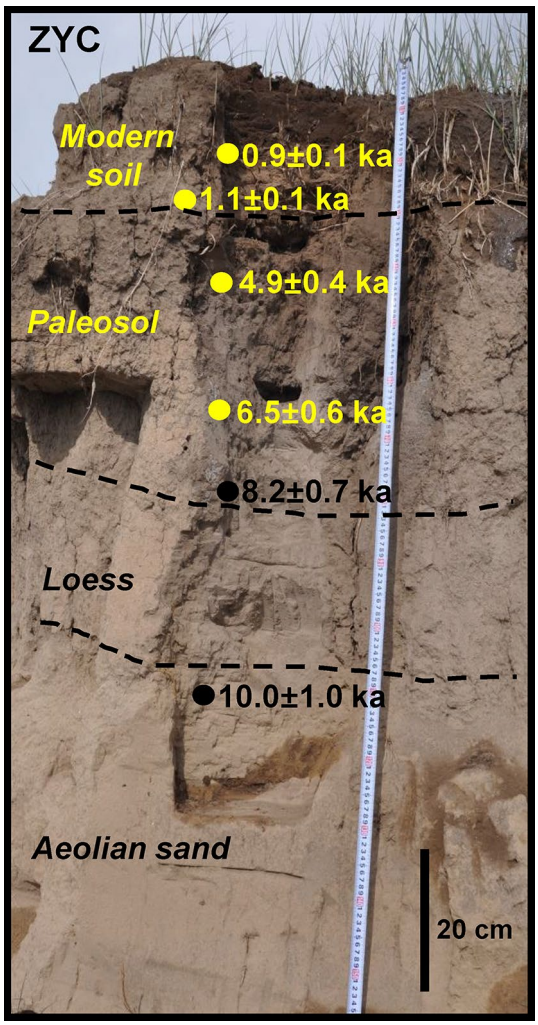

Fig. 2 ZYC section with the OSL ages (Zeng et al. 2017), for the details of the ages please see Table S1. Black and yellow dots represent OSL dating sample collection positions

1.0 m. The transition between the paleosol and lower loess is gradual with an ambiguous boundary (Fig. 2). The loess and paleosol are relatively firm and compact, containing numerous pores and fibrous plant roots. Loose aeolian sand is at least 1.0 m thick and continues downwards to an unknown depth. The top 1.2 m of the section was cleaned for sample collection. Six samples for OSL dating and six bulk sediment samples for radiocarbon dating were collected from the section. Sixty samples for proxy analyses were taken at 2-cm intervals.

The chronologies of the ZYC section were already published by Zeng et al. (2017), which included both ^{14}C and OSL ages. The OSL ages are more reliable than ^{14}C ages, this study only uses the OSL ages (Fig. 2). The proxy samples were firstly air dried, then carefully disaggregated by hand. Magnetic susceptibility (MS) were measured using a Bartington Instruments magnetic susceptibility meter. Total organic contents (TOC) were analyzed on a Vario Pyro Cube Elemental Analyzer after carbonates were removed by dilute hydrochloric acid at the State Key Laboratory of Isotope Geochemistry, Guangzhou Institute of Geochemistry, Chinese Academy of Sciences. Bulk sediments were dried and sieved to obtain < 75 μm fraction, then sufficient amount of sediments in each sample were analyzed for sedimentary elemental concentrations on an Axios advanced wavelength dispersive X-ray fluorescence spectrometer (XRF) at the Qinghai Institute of Salt Lakes, Chinese Academy of Sciences (ISLCAS).

For grain size analysis, about 2 g sediments were soaked into H_2O_2 and HCl to remove organic matter, carbonate, and iron oxides, and were then dispersed with 10% $(NaPO_3)_6$ in an ultrasonic bath. Finally, the grain size distribution was measured by a Malvern 2000 laser diffraction instrument that ranging from 0.02 to 2000 μm at the Physical Geography Lab of Taishan College.

Chronologies and proxy results

Sedimentary facies and OSL ages of ZYC and KTN sections show that paleosol formed during mid and late Holocene (at least from 6.5 to 1.1 ka) (Fig. 3). MS and TOC curves of ZYC and KTN sections emerged high plateau between 6.5 and 1.1 ka, implying that pedogenesis occurred at this environmental optimum period. GS data also show that fine grain dust increased during this period (Fig. 3), suggesting a long distance dust transportation and remote dust source regions. In contrast, aeolian sands deposited during early Holocene (from 12 to 9 ka) and the last 1.1 ka, MS and TOC were low, GS became coarse (Fig. 3). Sedimentary

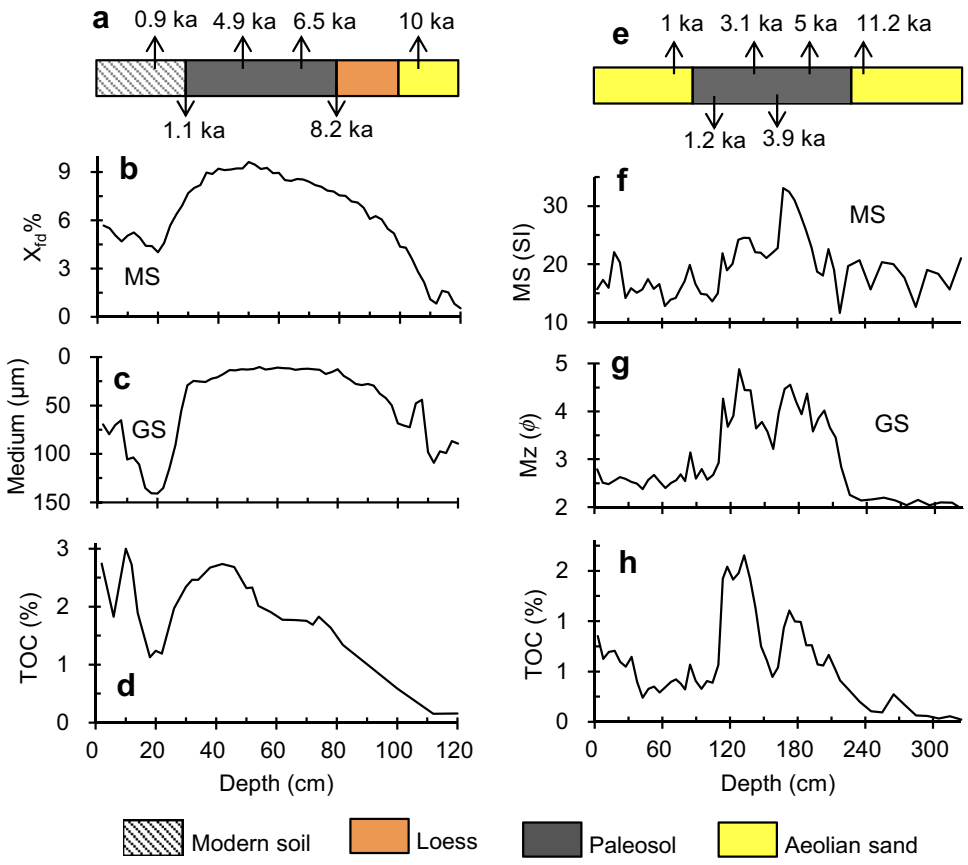

Fig. 3 Sedimentary facies diagram, magnetic susceptibility (MS), Grain size (GS, median) and Total organic content (TOC) curves of ZYC (left panel) and KTN (right panel)

structures show little or no evidence of pedogenic alteration, implying environmental condition was harsh and the source regions were relatively close for coarse grain aeolian sands and loess to deposit.

Figure 4 shows the comparison between the aeolian deposit ages and lake level fluctuation curve of Qinghai Lake since the last deglaciation. During lake lowstands (before 7 ka and since 1.1 ka), aeolian sands activated, indicating the occurrence or expansion of moving sands in eastern shore. However, during the lake highstands (7–3 ka and 2–1.1 ka), paleosol formed extensively and moving sands were largely stabilized in eastern shore (Fig. 4). Thus, it seems that the eastern shore aeolian activities were closely associated with the lake level fluctuations of upwind Qinghai lake during the Holocene epoch.

Coupled evolutions of Qinghai lake and its downwind aeolian sands

End-member decomposition of granular data

The ZYC and KTN aeolian sections are composed of similar strata: aeolian sands at the lower parts, and upward transit to loess and paleosol at the mid part, then modern soil or aeolian sands covered the top paloesol (Fig. 3).

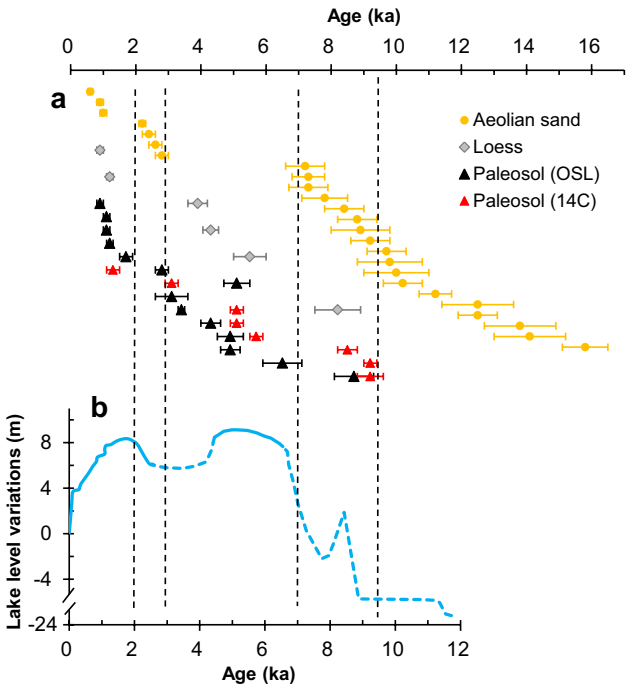

Fig. 4 **a** Plot of reported aeolian sediment ages from eastern shore deserts (Lu et al. 2010, 2015; Hu et al. 2012; Liu et al. 2012; Yang et al. 2018; Zeng et al. 2017); **b** The Holocene lake level variation curve of Qinghai Lake (Liu et al. 2015)

Both sites show that GS were coarse at aeolian sand layers, and GS became fine at loess and paleosol layers (Fig. 3). It is evident that the GS of KTN section are systematically coarser than ZYC section (Fig. 5). The GS distribution curves of aeolian sands contain only one coarse peak (centered at ~ 60 μm and ~ 120 μm for ZYC and KTN, respectively), indicating they are sorted quite well before deposition (Fig. 5a, c). The GS curves of loess show that they compose one fine GS peak (at ~ 15 μm and ~ 30 μm for ZYC and KTN, respectively) and another coarse GS peak (at ~ 60 μm and ~ 110 μm for ZYC and KTN, respectively) (Fig. 5a, c). The GS curves of paleosol show that they contain plenty of particles finer than 20 μm and 70 μm for ZYC and KTN sections, respectively (Fig. 5a, c).

End-member decomposition of GS data is effective in extracting information on provenance, transport processes, and the depositional environment of sediments (Zhang et al. 2017). Hence, we decomposed the GS data of ZYC and KTN sections using Bayesian End-Member Modeling Analysis (BEMMA) model (Yu et al. 2016). The grain size data of ZYC section can be decomposed to two end members: EM1 is similar to the aeolian sand, but even coarser than aeolian sand, EM2 is similar to the paleosol (Fig. 5b). The grain size data of KTN section can be decomposed to three end members, EM1, EM2 and EM3. They are similar to aeolian sand, paleosol and loess, respectively. The decomposed GS end-member curves are consistent with the lake level variation curve of Qinghai Lake: coarse grain sands increased when the lake level was low, and fine grain sediments increased during the lake highstands (Figs. 4, 6).

Pye and Tsoar (1987) proposed that particles greater than 50 μm were moved by wind as saltation, and can be transported up to ~ 30 km from the source region. In contrast, particles with diameter between 20 μm and 30 μm can be transported as far as 300 km by winds, and particles with diameter less than 20 μm can be transported to more than 1000 km as suspension. Therefore, we consider the coarse component (EM1) comes from adjacent source regions that are within 30–50 km upwind of the sandy lands, where the fine component (EM2) is largely from far range source regions that are 50–300 km upwind the Qinghai Lake. The decomposed grain size curves show that before ~ 9 ka and since ~ 1.1 ka, EM1 (the main particle size is 60–130 μm for ZYC and 100–500 μm for KTN, respectively) is the dominant component, and the EM2 (the main particle size is 3–40 μm for both ZYC and KTN) just constitutes a relatively small portion of the sediments (Fig. 6), implying mainly proximal source. However, during the mid and late Holocene (from ~ 7 to ~ 1.2 ka), EM2 is the dominant component, EM1 just contribute a small portion of sediments (Fig. 6), implying a distal source for the aeolian sediments.

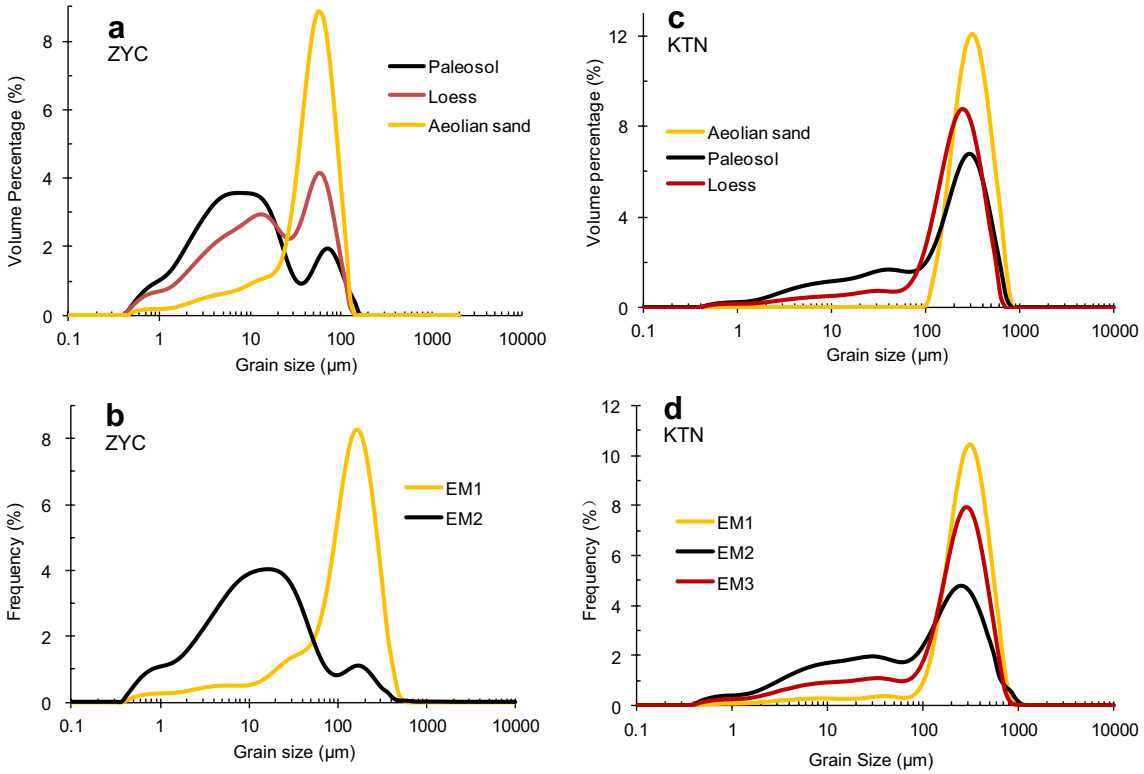

Fig. 5 Grain size distribution curves for aeolian sand, loess and paleosol of section ZYC (**a**) and KTN (**c**), and posterior distribution of the grain-size end-member spectra obtained using BEMMA for section ZYC (**b**) and KTN (**d**)

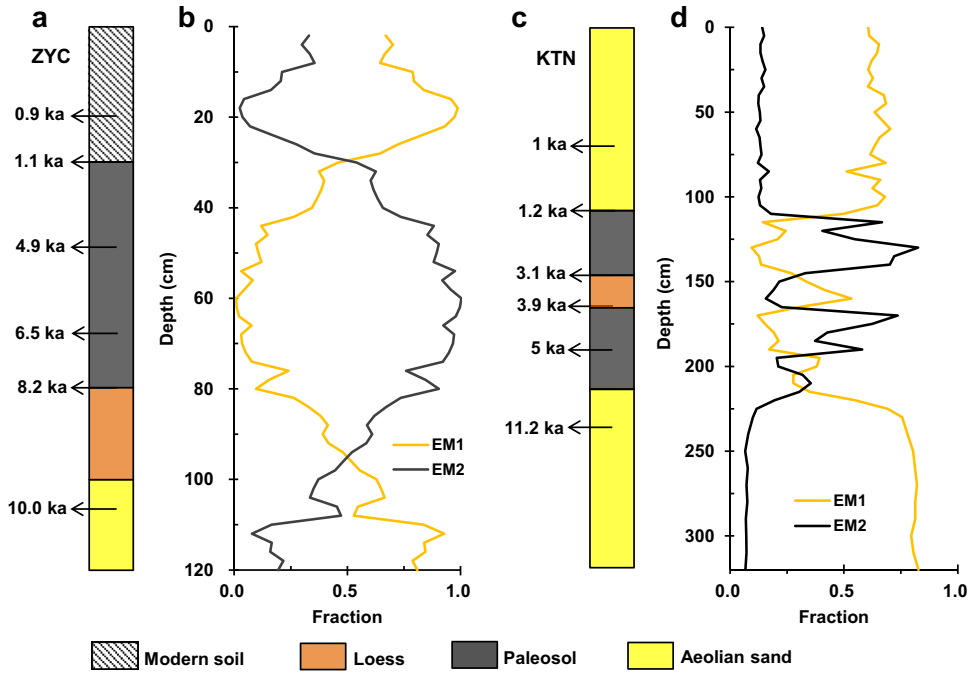

Fig. 6 Sedimentary facies diagram of section ZYC (**a**) and KTN (**c**), and changes in the fraction of the grain size end members with depth for section ZYC (**b**) and KTN (**d**). The ages for ZYC and KTN sections are cited from Zeng et al. (2017) and Lu et al. (2015), respectively

Elemental composition and sources

Al_2O_3, K_2O and TiO_2 contents of aeolian sediments increase as the sediments become fine, but they are not easy to migrate during weathering processes, so their ratios can be used to track the sediment sources (Gu 1999; Zeng 2017). Zr and Nb in sediments are relatively stable, and they preserve characteristics of source rocks, so they also can be used for provenance study (Zeng 2017). Zeng (2016) reported that the elemental molar ratio (K_2O/Al_2O_3, Zr/Ti, and Zr/Nb) in Qinghai Lake region can be used to distinguish aeolian sediments from fluvial and alluvial sediments, and he further proposed that loess in Qinghai Lake area mainly came from Qaidam Basin due to their similar K_2O/Al_2O_3, Zr/Ti, and Zr/Nb ratios. Hence, we analyzed element contents of aeolian sands, loess and paleosol of ZYC section using X-ray fluorescence spectrometer (XRF). The Zr/Ti against K_2O/Al_2O_3 and Zr/Nb against K_2O/Al_2O_3 were plotted in Fig. 7 for aeolian sands, loess and paleosol. The plots show that aeolian sands and paleosol can be separated by K_2O/Al_2O_3, Zr/Ti, and Zr/Nb ratios, whereas loess overlapped with both aeolian sands and paleosol (Fig. 7a, b). The plots indicate that elemental ratios of aeolian sands and paleosol fall within different ranges, suggesting they may have different source regions. This is in consistent with the GS data decomposition results. However, loess overlapped with both aeolian sands and paleosol, suggesting they may come from either paleosol or aeolian sand source regions, or a mixture of sediments from these two source regions.

Rb and Sr are easily fractionated during weathering processes on earth's surface due to Sr has much higher activity than relatively more inert behavior of Rb (Jin et al. 2015). Qinghai Lake catchment was dominated by carbonate weathering, and both Ca and Sr are readily transported into the lake in dissolved forms. The authigenic carbonate enriched lacustrine sediments in Qinghai Lake have low Rb/Sr and high Ca/Sr ratios, where terrestrial aeolian sediments show high Rb/Sr, but low Ca/Sr ratios (Jin et al. 2015) (Fig. 7c, d). The Rb/Sr ratios of sediments of ZYC section were higher than lacustrine sediments, fluvial sediments and surficial aeolian sediments surrounding the Qinghai Lake, implying that aeolian sediments experienced significant post-depositional chemical weathering. The highest Rb/Sr emerged from paleosol in ZYC section, suggesting that strong chemical weathering is an important part of the soil formation process (Fig. 7c, d).

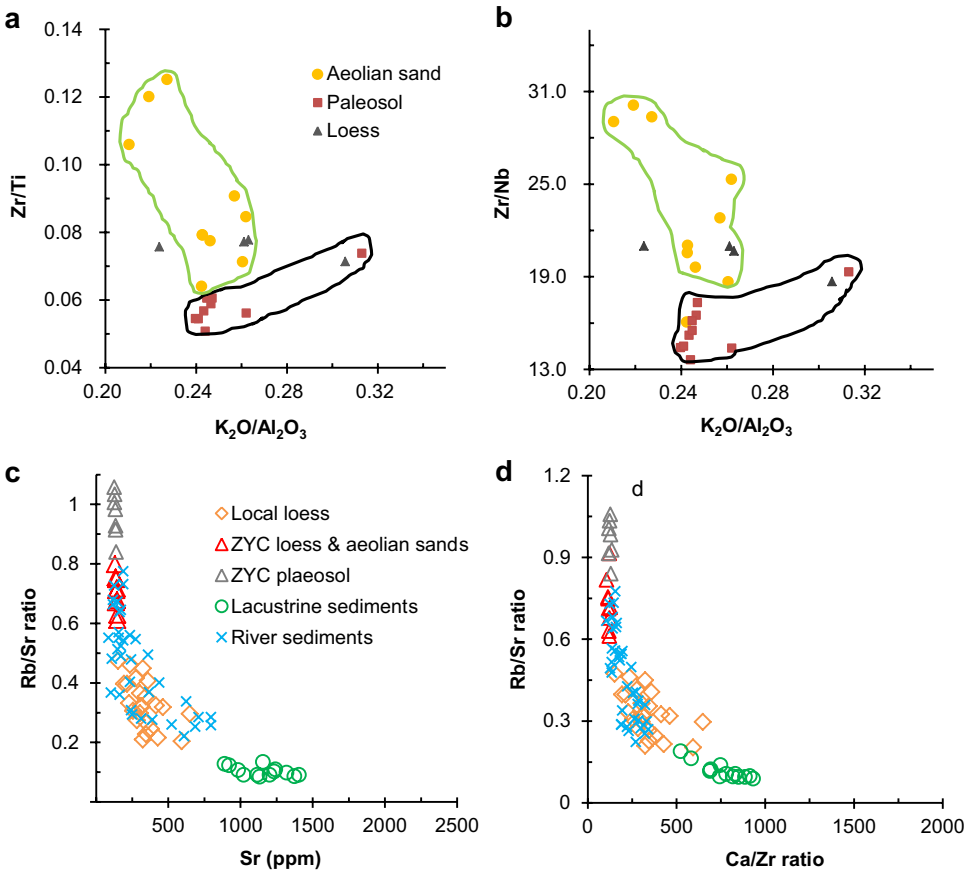

Fig. 7 Plots of element ratios. **a** K_2O/Al_2O_3 against Zr/Ti, **b** K_2O/Al_2O_3 against Zr/Nb for different aeolian sediments in ZYC section, **c** Rb/Sr ratios vs. Sr concentrations and Ca/Zr ratios (**d**)

Early and mid-Holocene lake and desert extension reconstruction

Early Holocene (11–9 ka) lacustrine sediments contain several layers of carbonate rich (mainly aragonite, calcite, and dolomite) silts and several layers of ruppia seeds and plant residues rich silts (Yu and Kelts 2002a). The authors interpreted that these ruppia seeds and plant residues were in situ deposited and preserved, not transported by lake water because there were no plant residues or ruppia seeds can be achieved from modern surface sediments taken from deep water areas in Qinghai Lake. They then deduced that the early Holocene Qinghai Lake was just several meters deep (at most 10 m). Recent lake drilling observations confirmed these early discoveries and their viewpoints (An et al. 2012; Liu et al. 2013; Jin et al. 2015; Li and Liu 2017).

In this study we use ASTER 30 m resolution DEM data, 1:200,000 topographic map and Arcgis 9.1 GIS software, to reconstruct the early to mid-Holocene lake extensions, and further tentatively inferred possible spatial extension of the eastern shore sandy lands during early Holocene lake lowstands. The isobaths of Qinghai Lake were first digitized from topographic map by hand, then the bathymetric image were generated by interpolating the vectorized isobaths data (Fig. 8a). The topographic map was produced at 1970, and the lake level of that year is approximately 3195 m above sea level (a.s.l.). Considering the early Holocene (11–9 ka) lake was ~ 10 m deep, the lake accumulated ~ 5 m detrital sediments during the Holocene (Shen et al. 2005; An et al. 2012; Wang et al. 2015), and the present maximum depth of the lake is ~ 30 m, hence we take 3170 m a.s.l. as the early Holocene lake level elevation, and obtained the early Holocene lake extension through spatial analyst tool (Fig. 8b). As the present eastern shore sandy lands distribute adjacent to the lake or even spread westward into the lake along the eastern lake margin, and westerly wind prevailed at present and since the last glaciation during winter and spring seasons (An et al. 2012; Zeng 2016). Therefore, we propose that during early Holocene lake lowstand, strong westerly wind would eroded the exposed lacustrine sediments that located at the west, north, and south sides of the lake and transported them to the eastern shore. The Tuanbao mountain and Riyue mountain prevented them from moving further eastward, caused the eastern shore sandy lands expanded, but still adjacent to the shrunk lake (like the present situation). The early Holocene lake extension and eastern shore sandy lands spatial ranges were then tentatively inferred (Fig. 8b).

The mid-Holocene lake extension were obtained according to the report that mid-Holocene lake level was ~ 9.1 m higher than present (Liu et al. 2015), using ASTER-DEM through spatial analyst tool (Fig. 8c). Although several researchers reported that the eastern shore sandy lands were largely stabilized and paleosol widely developed among sand

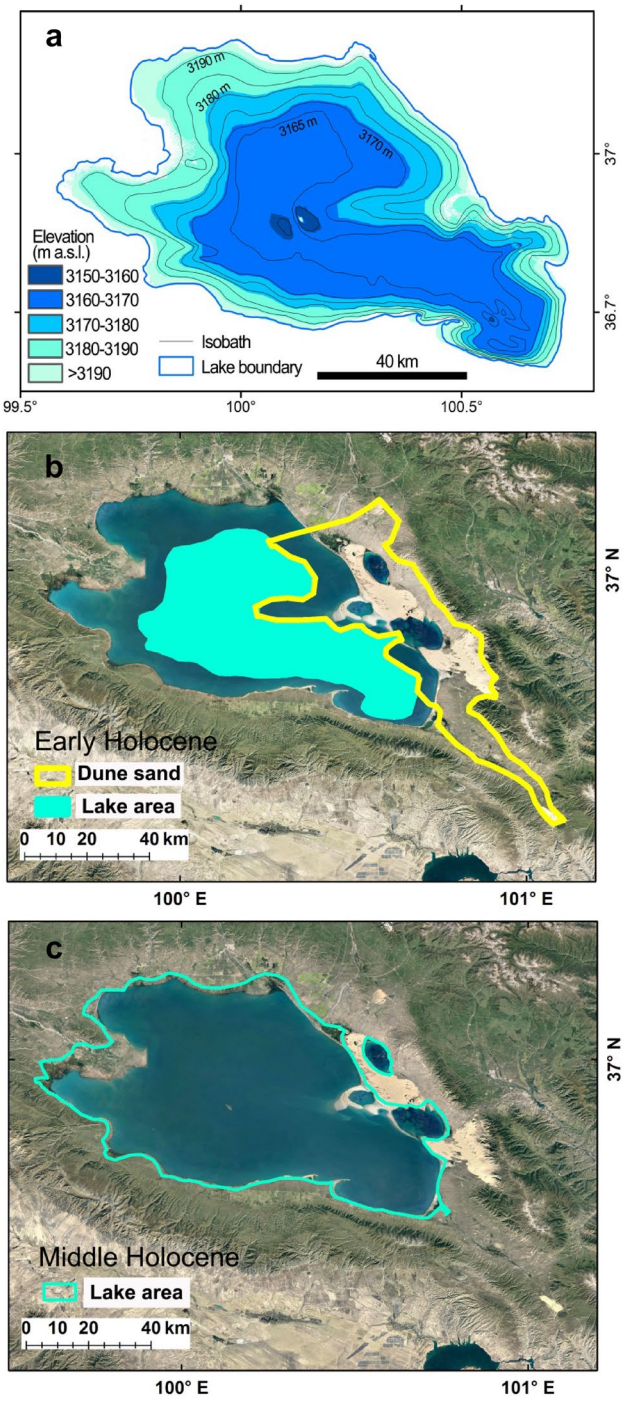

Fig. 8 Water depth map of 1970 (**a**) and tentatively reconstructed lake extensions of Qinghai Lake and eastern shore desert range for Early Holocene (**b**) and Mid-Holocene (**c**). The interval of isobaths in (**a**) is 5 m

dunes during mid to late Holocene (Lu et al. 2010, 2015, 2018; Liu et al. 2012; Hu et al. 2012), we also find paleosol developed and loess accumulated on top of early Holocene aeolian sands along the Daotang river valley, beyond the present sandy lands ranges. However, it is still difficult to

reconstruct the mid-Holocene eastern shore sandy lands spatial extension because enhanced aeolian activities during the recent millennia may destroyed or buried previously deposited loess and paleosol, although we are sure that the areas of eastern shore sandy lands shrunk greatly during mid-Holocene climate optimal period.

The relationship between Qinghai Lake and its downwind aeolian sediments

There are fundamental questions on when and how the eastern shore sandy lands formed and whether the aeolian sand evolutions coupled with the lake level fluctuations (or lake extension changes) of Qinghai Lake. Xu and Xu (1983) proposed that the formation of eastern shore sandy lands were associated with the recessions of the Holocene Qinghai Lake. When the lake shrunk, exposed lake bottom sediments were eroded by westerly winds and sands accumulated along the western piedmonts of Tuanbao Mount and Riyue Mount. Consequently eastern shore sandy lands formed. Moreover, previous studies suggest that the Qinghai Lake nearly dried up during the LGM (Chen et al. 1990; Shen et al. 2005; Jin et al. 2015), exposed vast areas of lake floors which suffered from drastic wind erosions, thereby causing medium to coarse sands accumulate at the eastern shore of the lake (Wang et al. 2017).

The TOC, MS, GS decomposition results and the elemental composition ratios in this study all are consistent with the lake level variations of Qinghai Lake during the Holocene epoch, therefore providing evidence for the connections between the lake extension changes and the eastern shore aeolian activities (Figs. 3, 4). Reconstructed early Holocene lake spatial extension suggested that vast areas of lake bottom were exposed, and provided potential materials for westerly wind to erosion and transportation (Fig. 8b). Hence, we propose that the aeolian sediments in eastern shore have both proximal and distal source. During the early Holocene, lake level was low, and vast ranges of lake floor exposed and was eroded by still stronger westerly winds, made the fine grain silts together with far range transported silts to be deflated and transported over the Riyue Mount to the Huangshui river terraces and western CLP (Liu et al. 2017), while coarse grain sands were accumulated at the western piedmont of Tuanbao mount and Riyue mount, and along the Dangtao river valley, caused the early Holocene eastern shore sandy lands spatial extension much larger than present (Figs. 8b, 9b). During the mid to early-late Holocene, the lake level was a few meters higher than present, and paleosol widely developed within eastern shore deserts, implying the deserts shrunk substantially, near distance source regions decreased, and the dust mostly came from long range transported silts from Qaidam basin that locate at the west-side of Qinghai Lake as Zeng (2016) proposed (Fig. 9a). During the past

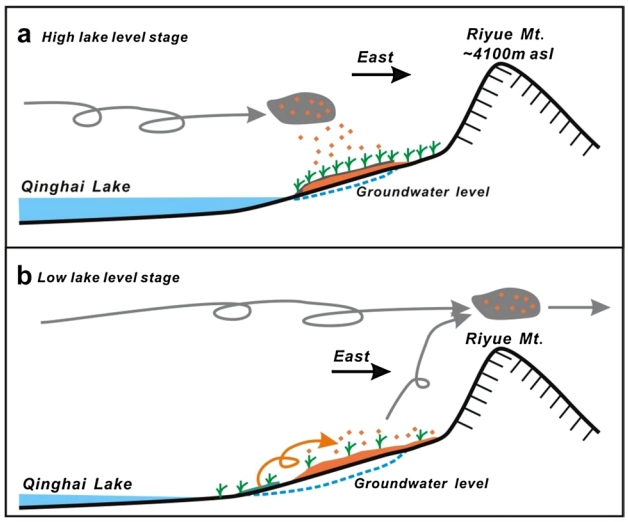

Fig. 9 Schematic diagrams for aeolian sediment accumulations at the eastern shore deserts. **a** during Holocene high lake level stages, long range transported dusts mainly deposited on the eastern shore; **b** during Holocene low lake level stages, exposed lacustrine sediments supply coarse sands to the eastern shore, while long ranges transported dusts and silts in lacustrine sediments were transported over the Riyue Mount to the Huangshui valley regions by westerly wind

~ 1.5 ka, lake level declined again, and the exposed lacustrine sediments provided parts of sands for eastern shore sandy lands, moreover, enhanced human activities degraded the grassland, therefore activating the sand and expanding the sand coverage (Yao et al. 2015).

Initial time of the aeolian sand

When the eastern shore aeolian sand initiated is also an intriguing question. We proposed that eastern shore aeolian activities were closely associated with Qinghai Lake water level variations during the Holocene epoch. The Qinghai Lake was formed ~ 4.6 Ma years ago (Fu et al. 2013), and the Quaternary climate changes were characterized by glacial–interglacial alternations. Thus it is not easy to determine when the eastern shore sandy lands initial formed. We know that the climate over northeastern QTP was cold and dry during the LGM, and loess deposited within the Qinghai Lake catchment were largely eroded and transported eastwards to Huangshui River basin and west part of CLP (Liu et al. 2017), and massive sand wedges formed on the northeastern QTP (Liu and Lai 2013). Meanwhile, Qinghai Lake shrunk to nearly dried up (Shen et al. 2005; Jin et al. 2015), and the eastern shore sandy lands expanded substantially (Wang et al. 2017). Hence, we are sure that the eastern shore sandy lands existed at least since the last glacial period. Whether the sandy lands initiated at the earlier cold-dry glacial stages is still unknown, and resolving this question relies on whether we can date the oldest aeolian sands that

deposited deeper underlie the present sand dunes or we can identify the oldest aeolian sediments from the drilled older lacustrine sediments as what Yuan et al. (1990) and Fu et al. (2013) did.

Implications for understanding the relationships between the lakes and aeolian sediments in QTP

There are more than one thousand lakes in the QTP, and most of them are inland closed lakes. These lakes are located at the lowest part of each drainage, as the sinks of the fine sediments eroded from surrounding mountains and highlands. On the other hand, lakes in this areas can be sources too. Previous studies reported that the QTP was dry and cold during the glacial stages, and lakes shrunk greatly. The exposed lacustrine sediments could be eroded and transported eastwards to supply materials for low altitude CLP and Sichuan Basin (Bowler et al. 1987; Fang 1995; Fang et al. 2004; Kapp et al. 2011; Pullen et al. 2011; Liu et al. 2017; Nie et al. 2015). During the interglacial stages, climate became warm and wet, lakes in QTP expanded, and loess accumulated on QTP (Bowler et al. 1987; Liu et al. 2012, 2015, 2017). Dong et al. (2016) reported that the dust spreading over the QTP were mostly derived from the erosion and the weathering of sediments and bedrocks within the plateau, and vast areas of deserts surrounding the QTP at the north and west sides supplied limited amounts of dust to the QTP. Moreover, many lakes besides Qinghai Lake have sandy lands distributed downwind of the lake, such as Haha Lake, Genggahai Lake, Donggi Cona Lake and Eling Lake (Stauch et al. 2012; Wünnemann et al. 2012; Qiang et al. 2014; Hu et al. 2017). This study suggests that downwind eastern shore sandy lands are closely coupled with the evolutions of upwind Qinghai Lake. In the future, investigating the relationships between the lakes and downwind aeolian sands in QTP other than Qinghai Lake are of important significances for resolving when and how the fine grain sediments in QTP were transported eastward to the CLP and Sichuan Basin, even to the Pacific Ocean (Fang et al. 2004), and also important for understanding the mass balance of the QTP in an uplifting background during the Cenozoic period.

Conclusions

Grain size, magnetic susceptibility, total organic contents, OSL ages and geochemical data of aeolian sediments along with lake level variations (or lake spatial extension changes) suggest that Qinghai Lake is closed associated with its downwind eastern shore sandy lands during the Holocene epoch. During low lake stands (11–9 ka), exposed lacustrine sediments provided materials for downwind sandy lands. However, during high lake level stages (7–1.2 ka), downwind eastern shore sands were largely stabilized with loess accumulations and paleosol formations.

The initial time of the eastern shore deserts is still unknown, but they have existed at least since the last glacial. During the LGM, Qinghai Lake nearly dried up, and the spatial coverage of eastern shore sandy lands were much larger than the early Holocene lowstand. This study also has important implications for future studies on the relationships between other lakes and their downwind sandy lands in QTP.

Acknowledgements This work was jointly funded by the National Natural Science Foundation of China (41671006) and the grant of Youth Innovation Promotion Association of CAS (2015350). Thanks to Prof. Ruijie Lu for providing data of KTN section, to Dr Luhua Xie and Professor Shuzhen Peng for measurements of TOC, MS and GS, to Derong Wang for XRF measurements and Fangming Zeng for useful discussion. Thanks two anonymous reviewers and the editor for their constructive suggestions that improved the quality of this paper.

References

An ZS, Colman SM, Zhou WJ, Li XQ, Brown ET, Timothy Jull AJ, Cai YJ, Huang YS, Lu XF, Chang H, Song YG, Sun YB, Xu H, Liu WG, Jin ZD, Liu XD, Cheng P, Liu Y, Ai L, Li XZ, Liu XJ, Yan LB, Shi ZG, Wang XL, Wu F, Qiang XK, Dong JB, Lu FY, Xu XW (2012) Interplay between the Westerlies and Asian monsoon recorded in Qinghai Lake sediments since 32 ka. Sci Rep 2:619. https://doi.org/10.1038/srep00619

Bowler JM, Chen KZ, Yuan BY (1987) Aspects of loess research-systematic variations in loess source areas: evidence from Qaidam and Qinghai Basins, Western China. China Ocean Press, Beijing, pp 39–51

Chen KZ, Bowler JM, Kelts K (1990) Paleoclimatic evolution within the Qinghai-Xizang (Tibet) Plateau in the last 40000 years. Quat Sci 1:21–31 **(in Chinese with English abstract)**

Chen FH, Wang SL, Zhang WX, Pan BT (1991) The loess profile at south bank, climatic information and lake-level fluctuations of Qinghai Lake during the Holocene. Scientia Geographica Sinica 11:76–85 **(in Chinese with English abstract)**

Chen FH, Wu D, Chen JH, Zhou AF, Yu JQ, Shen J, Wang SM, Huang XZ (2016) Holocene moisture and East Asian summer monsoon evolution in the northeastern Tibetan Plateau recorded by Lake Qinghai and its environs: a review of conflicting proxies. Quat Sci Rev 154:111–129

Dong ZW, Kang SC, Qin DH, Li Y, Wang XJ, Ren JW, Li XF, Yang J, Qin X (2016) Provenance of cryoconite deposited on the glaciers of the Tibetan Plateau: new insights from Nd–Sr isotopic composition and size distribution. J Geophys Res Atmos 121(12):7371–7382

Fang XM (1995) The origin and provenance of Malan loess along the eastern margin of Qinghai-Xizang (Tibetan) Plateau and its adjacent area. Sci China (Series B) 38(7):876–887

Fang XM, Han YX, Ma JH, Song LC, Yang SL, Zhang XY (2004) Dust storms and loess accumulation on the Tibetan Plateau: a case study of dust event on 4 March 2003 in Lhasa. Chinese Sci Bull 49(9):953–960

Fu CF, An ZS, Qiang XK, Bloemendal J, Song YG, Chang H (2013) Magnetostratigraphic determination of the age of ancient Lake Qinghai, and record of the East Asian monsoon since 4.63 Ma. Geology 41(8):875–878

Gu ZY (1999) Weathering histories of Chinese dust deposits based on Uranium and Thorium series nuclides, cosmogenic ^{10}Be, and major elements. Beijing: Ph.D Dissertation of Institute of Geology and Geophysics, Chinese Academy of Sciences, 1999, 1–99

Hu MJ, Li S, Gao SY, Zhang DS (2012) Evolution process of land desertification around Qinghai Lake since 32 ka BP reflected by sediment grain-size features. J Desert Res 32(5):1240–1247 **(in Chinese with English abstract)**

Hu GY, Yu LP, Dong ZB, Jin HJ, Luo DL, Wang YX, Lai ZP (2017) Holocene aeolian activity in the Headwater Region of Yellow River, Northeast Tibet Plateau, China: a first approach by using OSL-dating. Catena 149:150–157

Jin ZD, An ZS, Yu JM, Li FC, Zhang F (2015) Lake Qinghai sediment geochemistry linked to hydroclimate variability since the last glacial. Quat Sci Re 122:63–73

Kapp P, Pelletier JD, Rohrmann A, Heermance R, Russell J, Ding L (2011) Wind erosion in the Qaidam basin, central Asia: Implications for tectonics, paleoclimate, and the source of the Loess Plateau. GSA Today 21:4–10

Kelts K, Chen KZ, Lister G (1989) Geological fingerprints of climate history: a cooperative study of Qinghai Lake, China. Eclogae Geol Helv 82(1):167–182

Li XZ, Liu WG (2014) Water salinity and productivity recorded by ostracod assemblages and their carbon isotopes since the early Holocene at Lake Qinghai on the northeastern Qinghai–Tibet Plateau, China. Palaeogeogr Palaeocl 407:25–33

Li XZ, Liu WG (2017) Lake evolution and hydroclimate variation at Lake Qinghai (China) over the past 32 ka inferred from ostracods and their stable isotope composition. J Paleolimnol 58(3):299–316

Li XY, Xu HY, Sun YL, Zhang DS, Yang ZP (2007) Lake-level change and water balance analysis at Lake Qinghai, West China during recent decades. Water Resour Manag 21:1505–1516

Li XY, Ma YJ, Huang YM, Hu X, Wu XC, Wang P, Li GY, Zhang SY, Wu HW, Jiang ZY, Cui BL, Liu L (2016) Evaporation and surface energy budget over the largest high-altitude saline lake on the Qinghai-Tibet Plateau. J Geophys Res Atmos 121(18): 10,470–10,485

Li XZ, Liu XJ, He YX, Liu WG, Zhou X, Wang Z (2018) Summer moisture changes in the Lake Qinghai area on the northeastern Tibetan Plateau recorded from a meadow section over the past 8400 yrs. Global Planet Change 161:1–9

Liu XJ, Lai ZP (2013) Optical dating of sand wedges and ice-wedge casts from Qinghai Lake area on the northeastern Qinghai-Tibetan Plateau and its palaeoenvironmental implications. Boreas 42:333–341

Liu XJ, Lai ZP, Fan QS, Long H, Sun YJ (2010) Timing for high lake levels of Qinghai Lake in the Qinghai-Tibetan Plateau since the Last Interglaciation based on quartz OSL dating. Quat Geochronol 5:218–222

Liu XJ, Lai ZP, Yu LP, Sun YJ, Madsen D (2012) Luminescence chronology of aeolian deposits from the Qinghai Lake area in the Northeastern Qinghai-Tibetan Plateau and its palaeoenvironmental implications. Quat Geochronol 10:37–43

Liu WG, Li XZ, An ZS, Xu LM, Zhang QL (2013) Total organic carbon isotopes: a novel proxy of lake level from Lake Qinghai in the Qinghai–Tibet Plateau, China. Chem Geol 347:153–160

Liu XJ, Lai ZP, Madsen D, Zeng FM (2015) Last deglacial and Holocene lake level variations of Qinghai Lake, north-eastern Qinghai-Tibetan Plateau. J Quat Sci 30(3):245–257

Liu XJ, Xiao GQ, Li ECY, Lai XZ, Yu ZP, Wang LP Z (2017) Accumulation and erosion of aeolian sediments in the northeastern Qinghai-Tibetan Plateau and implications for provenance to the Chinese Loess Plateau. J Asian Earth Sci 135:166–174

Lu HY, Zhao CF, Mason J, Yi SW, Zhao H, Zhou YL, Ji JF, Swinehart J, Wang CM (2010) Holocene climatic changes revealed by aeolian deposits from the Qinghai Lake area (northeastern Qinghai-Tibetan Plateau) and possible forcing mechanisms. The Holocene 21:297–304

Lu RJ, Jia FF, Gao SY, Shang Y, Li JF, Zhao C (2015) Holocene aeolian activity and climatic change in Qinghai Lake basin, northeastern Qinghai–Tibetan Plateau. Palaeogeogr Palaeocl 430:1–10

Lu RJ, Liu XK, Lu ZQ, Chen L, Du J (2018) A new find of macrofossils of Picea crassifolia Kom. in early–middle Holocene sediments of the Qinghai Lake basin and its paleoenvironmental significance. Quat Res 90:310–320

Ma WL (1998) The history of Qinghai Province and Qinghai Lake. Qinghai People's Press, Xining **(in Chinese)**

Madsen DB, Ma HZ, Rhode D, Brantingham PJ, Forman SL (2008) Age constraints on the late quaternary evolution of Qinghai Lake, Tibetan Plateau. Quat Res 69:316–325

Nie JS, Stevens T, Rittner M, Stockli D, Garzanti E, Limonta M, Bird A, Andò S, Vermeesch P, Sayler J, Lu HY, Breecker D, Hu XF, Liu SP, Resentini A, Vezzoli G, Peng WB, Carter A, Ji SC, Pan BT (2015) Loess Plateau storage of Northeastern Tibetan Plateau-derived Yellow River sediment. Nat Commun 6:49–55

Pullen A, Kapp P, McCallister AT, Chang H, Gehrels GE, Garzione CN, Heermance RV, Ding L (2011) Qaidam Basin and northern Tibetan Plateau as dust sources for the Chinese Loess Plateau and paleoclimatic implications. Geology 39(11):1031–1034

Pye K, Tsoar H (1987) The mechanics and geological implications of dust transport and deposition in deserts with particular reference to loess formation and dune sand diagenesis in the northern Negev, Israel. Geol Soc Spec Pub 35(1):139–156

Qiang MR, Liu YY, Jin YX, Song L, Huang XT, Chen FH (2014) Holocene record of eolian activity from Genggahai Lake, northeastern Qinghai-Tibetan Plateau, China. Geophys Res Lett 41(2):589–595

Rhode D, Ma HZ, Madsen DB, Brantingham PJ, Forman SL, Olsen JW (2010) Paleoenvironmental and archaeological investigations at Qinghai Lake, western China: Geomorphic and chronometric evidence of lake level history. Quat Int 218:29–44

Shen J, Liu XQ, Wang SM, Matsumoto R (2005) Palaeoclimatic changes in the Qinghai Lake area during the last 18,000 years. Quat Int 136:131–140

Stauch G, Ijmker J, Pötsch S, Hilgers A, Diekmann B, Dietze E, Hartmann K, Opitz S, Wünnemann B, Lehmkuhl F (2012) Aeolian sediments on the north-eastern Tibetan Plateau. Quat Sci Rev 57:71–84

Wang HY, Dong HL, Zhang CL, Jiang HC, Liu ZH, Zhao MX, Liu WG (2015) Deglacial and Holocene archaeal lipid-inferred paleohydrology and paleotemperature history of Lake Qinghai, northeastern Qinghai-Tibetan Plateau. Quat Res 83:116–126

Wang Z, Liu XJ, Cong L (2017) Reconstruction of desert areas during Last Glacial Maximum and Early Holocene at the eastern side of Qinghai Lake. J Salt Lake Res 25(2):67–75 **(in Chinese with English abstract)**

Wünnemann B, Wagner J, Zhang YZ, Yan DD, Wang R, Shen Y, Fang XY, Zhang JW (2012) Implications of diverse sedimentation patterns in Hala Lake, Qinghai Province, China for reconstructing late quaternary climate. J Paleolimnol 48:725–749

Xu SY, Xu DF (1983) A primary observation of aeolian sand deposits on eastern shore of the Qinghai Lake. J Desert Res 3(3):11–17 **(in Chinese with English abstract)**

Yang LH, Long H, Cheng HY, He Z, Hu GY (2018) OSL dating of a mega-dune in the eastern Lake Qinghai basin (northeastern Tibetan Plateau) and its implications for Holocene aeolian activities. Quat Geochronol 49:165–171

Yao ZY, Li XY, Xiao JH (2015) Driving mechanism of sandy desertification around the Qinghai Lake. J Desert Res 35(6):1429–1437 **(in Chinese with English abstract)**

Yu JQ (2005) Qinghai Lake, China: a multi-proxy investigation on sediment cores for the reconstructions of paleoclimate and paleoenvironment since the Marine Isotope Stage 3. PhD Dissertation.

Faculty of Materials and Geoscience, Technical University of Darmstadt

Yu JQ, Kelts KR (2002a) Climatic change in the northeast Qinghai-Tibet Plateau during the late glacial/holocene transition. Quat Sci 22(5):413–423 **(in Chinese with English abstract)**

Yu JQ, Kelts KR (2002b) Abrupt changes in climatic conditions across the late-glacial/Holocene transition on the NE, Tibet-Qinghai Plateau: evidence from Qinghai Lake, China. J Paleolimnol 28:195–206

Yu SY, Colman SM, Li LX (2016) BEMMA: a hierarchical Bayesian end-member modeling analysis of sediment grain-size distributions. Math Geosci 48(6):723–741

Yuan BY, Chen KZ, Bowler JM, Ye SJ (1990) The formation and evolution of the Qinghai Lake. Quat Sci 3:233–243 **(in Chinese with English abstract)**

Zeng FM (2016) Preliminary Study on the Provenance of the Late Quaternary Loess Deposit in the Qinghai Lake Region. Earth Sci 14(1):1–8 **(in Chinese with English abstract)**

Zeng FM (2017) Element compositions of neogene eolian deposits in Xining area and their implication for provenance tracing. Quat Sci 37(6):1309–1319 **(in Chinese with English abstract)**

Zeng FM, Liu XJ, Li XZ, E CY (2017) Aquatic species dominate organic matter in Qinghai Lake during the Holocene: evidence from eolian deposits around the lake. J Earth Sci 28(3):484–491

Zhang PX, Zhang BZ, Qian GM, Li HJ, Xu LM (1994) The study of paleoclimatic parameter of Qinghai Lake since Holocene. Quat Sci 3:225–237 **(in Chinese with English abstract)**

Zhang XN, Zhou AF, Wang X, Song M, Zhao YT, Xie HC, Russell JM, Chen FH (2017) Unmixing grain-size distributions in lake sediments: a new method of endmember modeling using hierarchical clustering. Quat Res 89(1):365–373